

# Development of the RF Electronics Unit for NASA's Ecological Synthetic Aperture Radar

Martin L. Perrine, Rafael Rincon, Tamiola Fatoyinbo, Robert Zimmerman, Nicholas Spartana, Franklin Robinson, Paul James, Stephen Seufert, Michael Triesky, Kiara Beltran and Paul Fon

Flight Microwave and Telecommunication Systems  
NASA Goddard Space Flight Center  
Greenbelt, MD, USA  
martin.perrine@nasa.gov

**Abstract**—In its Carbon Cycle research efforts, prioritized by the National Science Foundation Decadal Survey and mandated by the US Congress, NASA is developing an airborne P-band Ecological Synthetic Aperture Radar called EcoSAR. By using polarimetric and interferometric techniques, and a digital beamforming phased-array architecture, EcoSAR will characterize biomass and ecological structure in three dimensions aboard a P-3 aircraft. One of the main components in the EcoSAR instrument development is the 32 channel RF Electronics Unit (REU). The multi-channel solid-state REU design provides amplification, conditioning, blanking, and several calibration schemes to meet EcoSAR's science and engineering requirements. The design, assembly, and testing of the REU is well underway with 16 of 32 channels completed. The remaining channels are nearly finished. The REU, once complete, will be calibrated and integrated with the rest of the system in preparation for EcoSAR's first flight campaign.

**Keywords**— SAR; Radar; polarimetry, interferometry, PolInSAR, transceiver; transmitter; receiver; array; wideband

## I. INTRODUCTION

The Ecological Synthetic Aperture Radar (EcoSAR) is an airborne P-band instrument being developed at NASA Goddard Space Flight Center [1],[2]. This effort is funded by the NASA Earth Science Technology Office's Instrument Incubator Program (IIP-10). EcoSAR builds on the recent successes of NASA's L-band Digital Beamforming SAR (DBSAR) instrument, which demonstrated advanced digital beamforming SAR techniques for surface imaging and biomass applications [3],[4],[5].

EcoSAR's full polarimetric and "single-pass" interferometric measurements will provide two- and three-dimensional fine-scale information of terrestrial ecosystem structure and biomass. See Fig. 1. These measurements directly support science requirements for the study of the carbon cycle and its relationship to climate change, recommended by the National Science Foundation's Decadal Survey [6] and highlighted in NASA's Plan for a Climate-Centric Architecture [7].

EcoSAR will operate at 435 MHz (69 cm wavelength), which allows the radar signal to fully penetrate vegetation structure and "sense" the entire canopy volume and wood density. The polarimetric backscatter measurements will provide the unique capability of mapping the forest cover; disturbance from

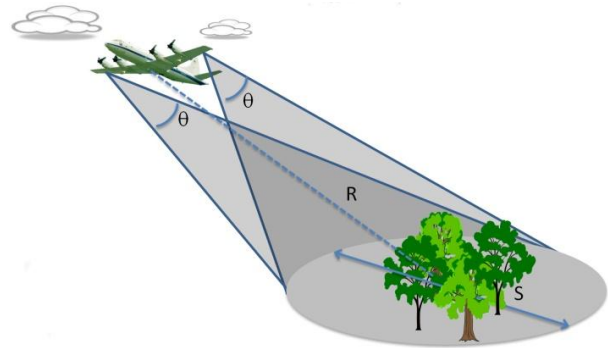


Fig. 1. EcoSAR's digital beamforming polarimetric and interferometric measurements will be used to characterize biomass and ecological structure in three dimensions from aboard a P-3 aircraft.

deforestation and degradation; forest recovery; wetland inundation; and above ground biomass. The "single-pass" Interferometric SAR (InSAR) and Polarimetric InSAR (PolInSAR) measurements will provide three dimensional vegetation structure [8], and biomass without any saturation [9]. EcoSAR's measurements are also desirable for several other critically important science measurements such as permafrost and ice dynamics which also support objectives outlined in the Decadal Survey.

## II. SYSTEM OVERVIEW

EcoSAR will employ a digital beamforming architecture comprised of reconfigurable digital waveform generators and receivers in the Digital Electronics Unit (DEU), high performance transceivers in the RF Electronics Unit (REU), and two wideband dual-polarization array antennas, as illustrated in Fig. 2. The antennas are mounted under the wings of a P-3 aircraft forming an interferometric baseline of 25 m (see Fig. 1). The chosen architecture will allow considerable measurement flexibility, including post processing synthesis of multiple beams, simultaneous measurement over both sides of the flight track, and variable incidence angle [2],[3]. Beams can be processed with different beamwidths and side lobe levels in order to control swath widths and minimize side lobe contamination. In-band interference in the receiver signal can be suppressed in post processing by appropriate null-steering of the antennas

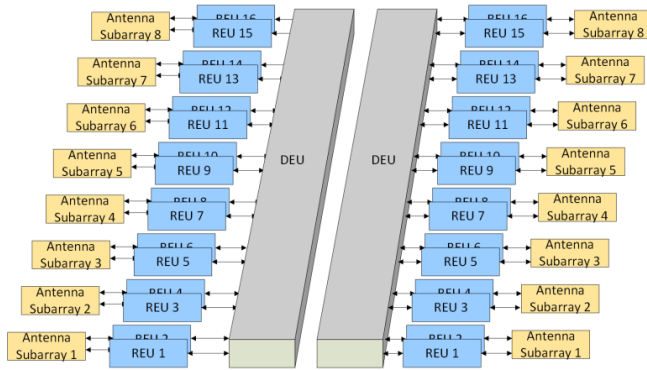


Fig. 2. EcoSAR's main subsystems consist of the Digital Electronics Unit (DEU), the RF Electronics Unit (REU), and the Antenna Array.

pattern. Adaptive signal equalization and predistortion is also supported. The instrument is intended to be used on the P-3 aircraft owned by NASA and NOAA.

The EcoSAR architecture will support full polarimetric operation by transmitting and receiving on both vertical and horizontal polarizations allowing the retrieval of the full backscattering matrix. A hybrid polarity mode is also supported that transmits with circular polarization, and receives horizontal and vertical polarizations. Orthogonal polarity waveform generation techniques will also be used to implement Radio Frequency Interference (RFI) mitigation techniques.

EcoSAR will feature a fully programmable bandwidth over a 200 MHz range for both bandwidth and spectral notching. This capability will allow the instrument to adjust the range resolution according to mission requirements in a heavily used P-band environment. Operational modes with slant range resolutions from 5 meters (30 MHz bandwidth) to 25 meters (6 MHz bandwidth) will be used as nominal modes in frequency restricted areas, and a science mode with slant range resolutions as fine as 0.75 m (up to 200 MHz bandwidth) will be employed in authorized or remote areas.

Key system characteristics are given in Table 1.

Center Frequency	435 MHz
Maximum Bandwidth	200 MHz
Polarization	HH, HV, VH, VV
Polarization Isolation	< -30 dB
Noise Equivalent $\sigma_0$ (from 8km)	- 42 dB (uniform illum.)
Total Number Channels	32
Interferometric Baseline	25 m
Pulse Length	1usec – 50usec
Array Peak Power	32 Watts (uniform illum.)
PRF	100 Hz – 10 KHz
Nominal Swath	4 km
Finest Range Resolution	0.75 m
Single Look Azimuth Resolution	0.5 m
Vertical Accuracy	< 5 m

TABLE 1 Key System Characteristics

### III. RF ELECTRONICS UNIT

The ECOSAR instrument requires 32 independent radar channels to fully support all functionality mentioned above. The primary function of the REU is that of a transceiver; to amplify the transmit signal to the necessary power level to feed the antennas and to amplify and condition the very low power radar return signal for processing. In addition, the transceiver must provide the means to calibrate both the transmitter and receiver, and to reject out-of-band interference for the receiver. The 32 transceivers combined with power, thermal control and signal distribution make up the REU.

#### A. Driving Considerations for the Transceiver:

Performance requirement:

The basic radar system requirement to meet is -42 dB noise equivalent sigma naught NESO ( $\sigma_0$ ) in 200 MHz BW with 12 dB signal to noise (s/n) ratio.

Basic starting assumptions:

The transceiver electronics will be located in the fuselage, away from the antennas located on the wing tips. This simplifies the overall design and relaxes size, power, and thermal constraints, but at the cost of degraded sensitivity due to the high loss of long cable lengths.

To minimize size and maximize performance, the project started out with the idea to build the transceiver based on a printed circuit board hosting a 10W power amplifier.

#### B. Design:

Approach:

The necessity of building and maintaining 32 channels prompted the team's desire to simplify the design as much as possible. Therefore, the team decided to:

- Avoid up and down conversion since current analog-to-digital and digital-to-analog chips allow direction operation at 435 MHz.

- Simplify RF design by pushing the basic functions of modulation, and amplitude and phase control to the digital domain. Additionally, in-band hardware requirements that are normally very stringent can be relaxed if advanced digital processing techniques are employed to compensate for channel distortions, such as adaptive equalization for receive and adaptive predistortion for transmit.

- Utilize commercial parts to the extent possible. Modest development effort was considered acceptable.

- Incorporate methods to simplify construction and maintenance, early in the design.

- Address thermal as well as electromagnetic interference (EMI) and electromagnetic compatibility (EMC) considerations early in the process, which greatly influenced the design.

- Use a commercial manufacturer and software to design, lay out and build the receiver printed circuit board (PCB).

- Provide separate calibration for transmit and receive paths.

### Commercial Component Survey:

A market survey was performed to identify the critical long lead parts. The survey quickly identified that:

- 200 MHz BW P-band circulators were not available but could possibly be developed with low risk.
- 5W units were available in surface mount packages.
- 20W power amplifiers were available in coaxial packages but low cost units may require equalization and predistortion.
- It may be possible to develop a 20W amplifier with fast turn-off capability with medium risk and modest cost.
- 20W peak pin diode switches could be developed with low risk.
- Low noise amplifiers and bi-directional couplers were available.
- High performance RF cables typically go up to 18 GHz and may be overkill for operation at P-band. A lower cost approach might be possible at these frequencies but stability would have to be evaluated.

The findings from the survey prompted several key design decisions. Ten Watt surface mount components were not available "off the shelf"; this necessitated a choice between a lower power PCB version and a higher power version using coaxial components. Performance was considered most important, so the coaxial option was selected. The selection of coaxial components allowed migration to a higher power solution (20W rather than 10W), and thus higher sensitivity. Secondly, 20W transmit or receive (T/R) switches were feasible and would provide better performance than a

circulator. Thirdly, coax components allowed more options to address thermal dissipation.

There was still a desire to minimize size and simplify construction, so a hybrid approach was chosen: the low power components (receiver, calibration and Transmit driver) were placed on a micro-strip printed circuit board, and the high power components were coaxial.

### Component Development:

Based on the market survey results, NASA sought multiple contracts to build prototype circulators, switches and power amplifiers with 200 MHz BW and 20W power handling. Through these contracts, two circulators, three T/R switches, and three amplifiers were developed. One of the amplifiers had fast turn on/off that would lower average power and reduce transmit noise leakage during receive. These components were used to build a prototype transceiver.

The circulator and switches for the final operational system were purchased through a competitive process. The team chose the amplifier with the switched capability to reduce noise and thermal dissipation. The REU design was done in a conservative fashion however, such that the fast switching, though beneficial, was not required.

### Transceiver design:

The conceptual block diagram is shown in Fig. 3. The transmit path was designed accounting for dynamic range, impedance matching and signal levels. A driver amplifier was required to boost the signal from the signal generator. Noise leakage from the power amplifier into the receive path was found to be high and a blanking switch was added. With this switch in place it was easy to add a point to directly monitor

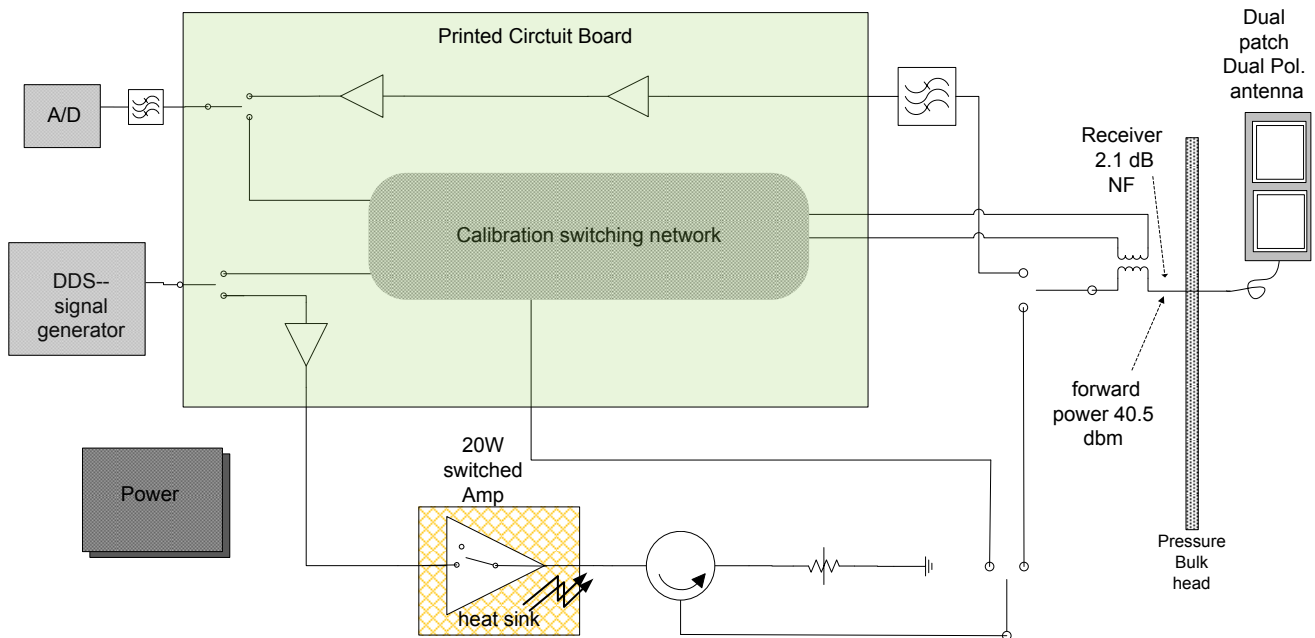


Fig. 3 Conceptual REU block diagram.

the power amplifier. A bidirectional coupler was added to monitor the forward and reverse signals at the antenna port.

The receive path was designed in a similar fashion but noise figure and out-of-band rejection had to be considered. A coaxial filter was used for adaptation to future spectral environments. A receiver calibration signal was injected through the coupler.

A switching network was added to interconnect the three transmit monitor points and the receive calibration path to the signal generator and the A/D receiver.

In addition to the receive path components, the receiver board contains all low power switches, a transmit signal drive amplifier, and transistor transistor logic (TTL) switch control drivers. The interface of the TTL switch control signals with the processor is via RS 486 differential signal format. The final PCB is built on a four-layer board made with 370HR and is shown mounted in its EMI enclosure in Fig. 4.

During the design process, a simple component test board was made to demonstrate and select the critical receiver components. A prototype receiver board was then designed and built using the final components. A prototype transceiver was then built by integrating the prototype PCB and coaxial components to validate the overall transceiver design.

#### EMI/EMC:

Design review and consultation with NASA/GSFC's EMC working group was made at the prototype stage. Updates to the receiver design were made as a result. When considering how to integrate the 32 transceivers, a conservative approach was taken to enhance electrical isolation. At the cost of size, each channel was physically isolated rather than combining them into a single chassis. Coaxial components were kept external to the receiver box to provide physical access and heat removal. Once the first unit was built, however, comprehensive shielding proved difficult due to the use of solder pins on the active components.

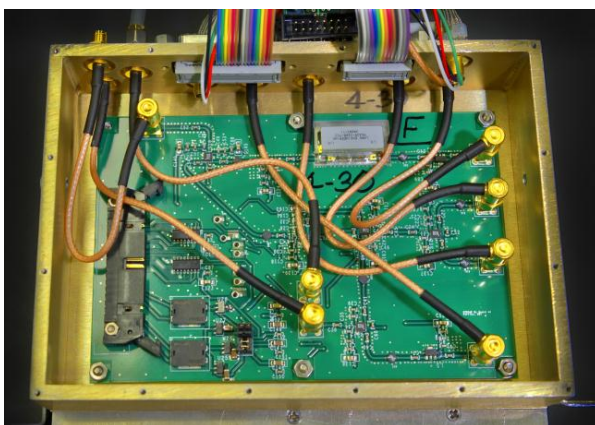


Fig. 4 Receiver PCB in enclosure with cabling.

In hindsight, doing the following would have facilitated shielding of power and control lines: first, integrating the receiver board and coaxial components into the same chassis; and second, using shielded connectors rather than solder pins on the RF components that have power and control lines.

#### Mechanical Design:

The driving considerations for the mechanical design were as follows:

- 1) Physical mounting and vibration isolation.
- 2) Physical isolation of each channel for EMC/EMI purposes.
- 3) Heat dissipation from the power amplifier.
- 4) Physical access to facilitate interconnection, testing and maintenance.
- 5) Use of standard aircraft equipment racks.
- 6) Migration to a more compact housing in the future.

There were numerous options to choose from for physical layout of the transceiver channel. The design shown in Fig. 5 was chosen because it addressed the driving considerations. The power amplifier was mounted on an isolated heat sink to facilitate heat removal. The PCB was mounted in a small chassis to provide shielding and mechanical protection. The coaxial components were mounted on the back side of the receive box to allow access while minimizing space and to simplify interconnection. The receive box was placed at a triangular orientation providing a simple but secure way to mount the hardware. The overall space needed is reduced with this configuration, yet there is still physical access to the power amp and the coax components.

Typical power amplifiers are about 15% efficient, therefore, subsystem power dissipation was expected to be up to 4300 Watts (32 channels at 20W RF corresponding to 133W DC

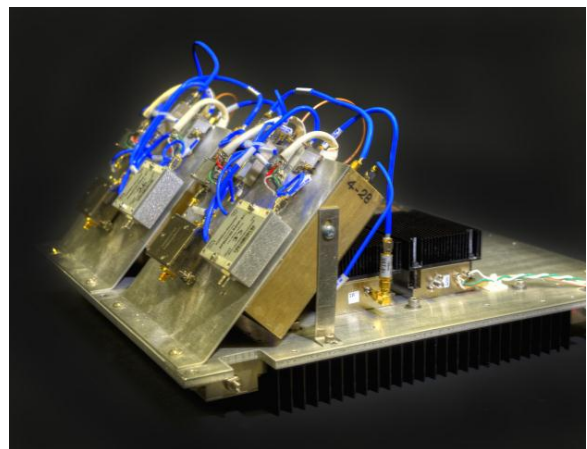


Fig. 5 Transceiver channel showing coaxial components mounted on back of receive box over the power amplifier. Primary heat sink is shown on the bottom of the tray and secondary heat sink is shown on top of the amplifier



power per channel). Due the large anticipated dissipation, the thermal design was addressed early on but, changed considerably throughout the process. Initially, a liquid cooled approach that NASA was developing for space-borne electronics was considered. This concept used a novel electrohydrodynamic (EHD) pump that moved heat from the power amplifier to a liquid reservoir through micro-tubes. This heat would then be transferred to a heat sink outside the fuselage with a conventional pump. Complexity was an issue. A second more conventional liquid-cooled approach was also considered using a standard cooler. However, the large power draw was concerning. Late in the design process it was determined that the aircraft air cooling system could handle the instrument's thermal load and a simpler approach using air convection was chosen.

For convenience, a thermal tray was designed with a common heat sink that hosts four transceiver channels. In addition, small individual heat sinks are mounted on the top side of each power amp as shown in Fig. 5. Two of these thermal trays are vertically mounted on each side of an equipment rack which hosts the 16 transceiver channels needed to drive the array antenna on one wing. The primary heat sinks are mounted vertically and in a fashion where the cooling volume is shared between the four trays. The receiver box triangular mounting structures are oriented in a manner that creates a vertical tunnel for airflow over the secondary heat sinks. Two banks of fans are used to move the air over the structure, one at the top and one at the bottom, as shown in Fig. 6. Only the front 8 channels are seen in the figure. Thermal sensors are placed near each power amplifier and are monitored via computer software which controls the fans to stabilize operating temperature.

### C. Status

The status of the RF Electronics Unit build is summarized below.

The first of two flight racks, which hosts 16 transceiver channels, has been fully integrated and wired. The unit has been tested on a channel by channel basis with RF switches in a static configuration. Receiver noise testing is pending.

A dynamic switch control test of each transceiver has been performed on the bench. A similar test of the entire rack is pending completion of the system controller firmware. This test will include full power operation, timing check, and a long-term thermal "bake-in".

Two of the four trays needed for the second rack have been built and bench-tested, while the last two trays are being built at the time of writing this paper.

The REU is scheduled to be integrated with the system late in the summer of 2013. The array antennas and DEU are in the final phases of their build. Firmware development is progressing for the DEU. Testing and calibration are scheduled in preparation for flight tests and two field campaigns in the 2013/2014 time frame.

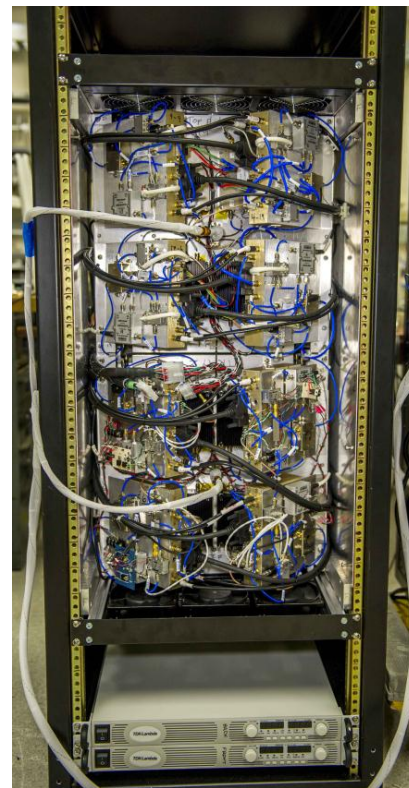


Fig. 6 First integrated rack of 16 transceivers, eight are visible.

### D. Test to Date

Prior to integration of the channel into the rack, a dynamic switch-controlled test was implemented using a radar processor unit built for the DBSAR instrument, the predecessor to EcoSAR. This test activated each operational mode and then each switch one at a time while triggering a pulse from a conventional pulse generator. The output was displayed on a spectrum analyzer in a "zero span" mode. The results are of amplitude versus time of the calibration path and can be compared to a template of expected levels, Fig. 7. This test provided an efficient means to functionally test all components in a transceiver channel. The sharp spikes at the start or end of the noise pedestals are switching transients that occur outside of the transmit and receive windows. Switch 7 could not be cycled in the test mode to protect the low-noise amplifier (LNA) from large signal transients. The noise levels during both receive and calibration periods are seen. A receive window occurs between each transmit pulse and a corresponding test through the receive

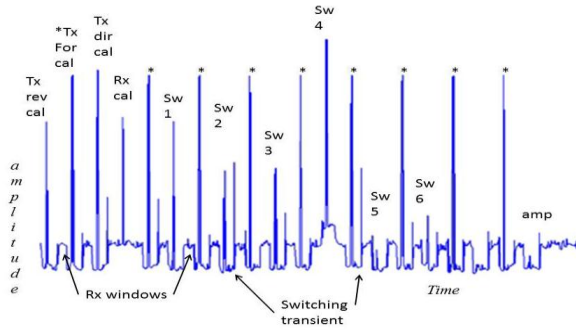


Fig. 7 Example dynamic test output for the calibration path in a zero span spectrum analyzer display showing amplitude versus time for the four operational modes plus toggling of each of 7 switches.

path was made showing a received pulse during this time window.

S-parameter measurements for a representative transceiver are shown in Figs. 8 through 12. Figs. 8 and 9 show a one dB compression point versus power measurement of magnitude and phase deviation of the transmit path. Results at three frequencies across the band were taken. A summary of the results is given in Table 2. These full-power measurements were made with a high power attenuator in-line and calibrated out.

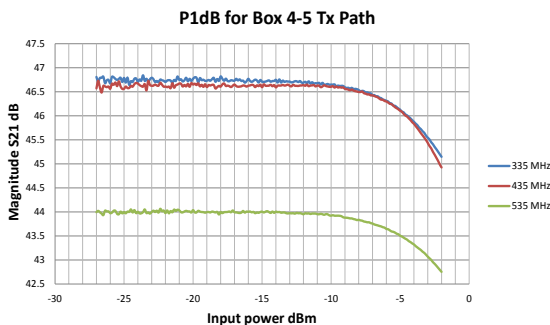


Fig. 8 Transmit path S21 magnitude versus power at three frequencies for one transceiver.

S21 phase normalized for Box 4-5 tx path

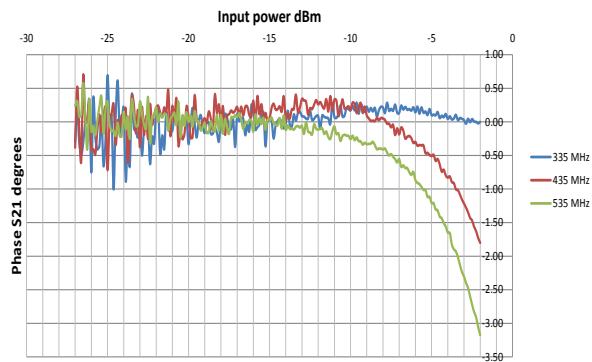


Fig. 9 Transmit path S21 phase versus power at three frequencies for one transceiver.

TABLE 2 Summary of Transmit Path Compression Measurement at P1dB

Frequency	Input level dBm	Gain (dB)	Output dBm	Phase Deviation Deg.
335 MHz	-3.50	45.72	42.22	0.10
435 MHz	-3.38	45.59	42.22	-1.02
535 MHz	-2.75	43.00	40.25	-2.47

Magnitude of S21 and S22 swept across the band is shown in Fig. 10. The low power test setup did not include the in-line attenuator mentioned above. The blue line shows the results taken at  $-5$  dBm, an input level close to the P1 dB points using the high power test setup.

S21 Phase deviation from a linear phase trend taken with  $-5$  dBm input signal is shown in Fig. 11.

Finally, receive path magnitude of S21 and S11 is shown in Fig. 12.

#### IV. SUMMARY

The RF Electronics Unit for the EcoSAR instrument built at NASA/Goddard Space Flight Center, for its surface imaging and biomass Earth Science airborne program, is reviewed in detail including measurement results. The subsystem design has been validated by measurement. The first 16 of 32 channels have been integrated and are being tested. The second set of 16 channels are being built and will be integrated and tested. The EcoSAR project plans to integrate, test and calibrate the full system for test and mission flights on the NOAA P-3 this fall and winter.

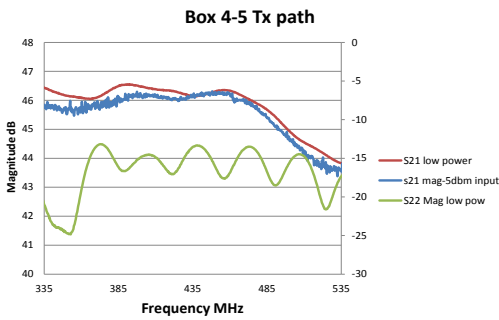


Fig. 10 Transmit path S21 and S22 magnitude versus frequency for two power levels.

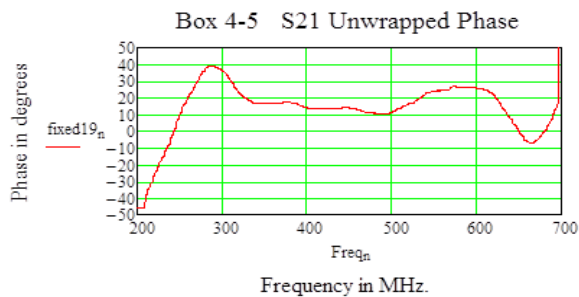


Fig. 11 Transmit path S21 phase deviation from linear trend vs frequency.

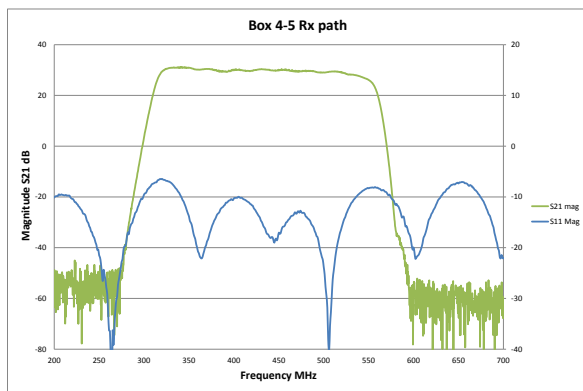


Fig. 12 Receive path S21 and S11 magnitude versus frequency.

#### REFERENCES

- [1] Fatoyinbo T., R. Rincon, G. Sun, K. J. Ranson, "EcoSAR: a P-band Digital Beamforming Polarimetric Interferometric SAR instrument to measure ecosystem structure and biomass", Proc. IEEE Int. Geosci. Rem. Sens. Symp., July 25-29, 2011, Vancouver, Canada.
- [2] Rincon, R. F. T Fatoyinbo, K J Ranson, G Sun, M Deshpande, R D Hale, A Bhat, M Perrine, C F Du Toit, Q Bonds, V Marrero, and P James. "Development of the EcoSAR P-band synthetic aperture radar". Proc. IEEE Int. Geosci. Rem. Sens. Symp., July 22-27, 2012, Munich, Germany.
- [3] Rincon, R. F.; Vega, M. A.; Buenfil, M.; Geist, A.; Hilliard, L.; Racette, P.; 2011A, "NASA's LBand Digital Beamforming Synthetic Aperture Radar," Geoscience and Remote Sensing, IEEE Transactions on, vol.49, no.10, pp.3622-3628, Oct. 2011 doi: 10.1109/TGRS.2011.2157971.
- [4] Rincon, R. F., T Fatoyinbo, J Ranson, G Sun, M Perrine, Q Bonds, S Valett, and S Seufert (2012). Digital Beamforming Synthetic Aperture Radar (DBSAR) polarimetric operation during the Eco3D flight campaign. Proc. IEEE Int. Geosci. Rem. Sens. Symp., July 22-27, 2012, Munich, Germany.
- [5] Rincon, R. M. Vega, M. Buenfil, A. Geist, L. Hilliard, and P. Racette, "DBSAR's First Multimode Flight Cam-paign", 2010 European Radar Conference, EUSAR 2010.
- [6] Earth Science and Applications from Space: National Imperatives for the Next Decade and Beyond. Committee on Earth Science and Applications from Space: A Community Assessment and Strategy for the Future, National Research Council (ESDS, 2007).
- [7] Responding to the Challenge of Climate and Environmental Change: NASA's Plan for a Climate-Centric Architecture for Earth Observations and Applications from Space, June 2010
- [8] S. R. Cloude and K.P. Papathanassiou, "Polarimetric SAR interferometry," Geoscience and Remote Sensing, IEEE Transactions on, vol. 36, no. 5, pp. 1551–1565, Sep. 1998.
- [9] M. Neumann, S. S. Saatchi, L. M. H. Ulander, and J. E. S. Fransson, "Assessing performance of L- and P-band polarimetric interferometric SAR data in estimating boreal forest above-ground biomass," IEEE Trans. Geosci. Remote Sens., vol. 50, no. 3, pp. 714–726, Mar. 2012.